International Journal of Nanomedicine

Dovepress
open access to scientific and medical research

Open Access Full Text Article

ORIGINAL RESEARCH

Crystalline and Amorphous Preparation of Aluminum Hydroxide Nanoparticles Enhances Protective Antigen Domain 4 Specific Immunogenicity and Provides Protection Against Anthrax

This article was published in the following Dove Press journal:
International Journal of Nanomedicine

Himanshu Gogoi[1]
Rajesh Mani[1]
Soumya Aggarwal[2]
Anshu Malik[1]
Manoj Munde[2]
Rakesh Bhatnagar[1,3]

[1]Laboratory of Genetic Engineering and Molecular Biology, School of Biotechnology, Jawaharlal Nehru University, New Delhi, India; [2]School of Physical Sciences, Jawaharlal Nehru University, New Delhi, India; [3]Banaras Hindu University, Varanasi, Uttar Pradesh, India

Introduction: Aluminum salts, although they have been used as adjuvants in many vaccine formulations since 1926, exclusively induce a Th2-biased immune response, thereby limiting their use against intracellular pathogens like *Mycobacterium tuberculosis*.

Methods and Results: Herein, we synthesized amorphous and crystalline forms of aluminum hydroxide nanoparticles (AH nps) of 150–200 nm size range. Using *Bacillus anthracis* protective antigen domain 4 (D4) as a model antigen, we demonstrated that both amorphous and crystalline forms of AH nps displayed enhanced antigen D4 uptake by THP1 cells as compared to commercial adjuvant aluminum hydroxide gel (AH gel). In a mouse model, both amorphous and crystalline AH nps triggered an enhanced D4-specific Th2- and Th1-type immune response and conferred superior protection against anthrax spore challenge as compared to AH gel. Physicochemical characterization of crystalline and amorphous AH nps revealed stronger antigen D4 binding and release than AH gel.

Conclusion: These results demonstrate that size and crystallinity of AH nps play important roles in mediating enhanced antigen presenting cells (APCs) activation and potentiating a strong antigen-specific immune response, and are critical parameters for the rational design of alum-based Th1-type adjuvant to induce a more balanced antigen-specific immune response.

Keywords: aluminum hydroxide gel, crystalline nanoparticles, NLRP3 inflammasome, Th1/Th2 immune response, amorphous nanoparticles

Introduction

Anthrax, a zoonotic disease, is caused by the etiological agent *Bacillus anthracis*, which is Gram-positive, rod-shaped and spore-forming. The virulence of *B. anthracis* is encoded by two plasmids, namely, pXO1 and pXO2. The plasmid pXO1 encodes for the tri-partite exotoxins, namely protective antigen (PA), lethal factor (LF) and edema factor (EF). All of these toxin components are non-toxic when they are alone. However, the toxin PA in combination with toxin LF gives rise to a lethal toxin which cleaves various mitogen-activated protein kinase kinases (MAPKKs),[1,2] resulting in the inactivation and disruption of various cellular signal transduction pathways[1,3] and causes lethality in experimental animal models. In combination, toxin EF with PA

Correspondence: Rakesh Bhatnagar
Banaras Hindu University, Room No. 102, New Delhi, India
Email rakeshbhatnagar@jnu.ac.in

submit your manuscript | www.dovepress.com
DovePress
http://doi.org/10.2147/IJN.S219647

forms edema toxin, which causes a rise in intracellular cyclic adenosine monophosphate (cAMP) level and multicellular bleeding in the host animal.[1,4,5] Toxin PA consists of 4 domains and domain 1 (residues 1–258) contains the furin cleavage site. Domain 2 (259–487) and domain 3 (488–595) are involved in heptamerization and pore formation through which LF/EF are translocated into the cytosol. Domain 4 is the most immunogenic and binds to tumor endothelial marker-8 (TEM8) and capillary morphogenesis gene-2 (CMG2), the only two known cellular receptors of anthrax toxin, and has been shown to provide protection against anthrax spore challenge.[6] The other plasmid, pXO2, encodes for the anti-phagocytic poly-D-glutamic acid capsule for *B. anthracis*.

Post-exposure therapeutics against the disease anthrax involves various antibiotics, namely doxycycline, ciprofloxacin, levofloxacin, and parenteral procaine penicillin G. However, it has been observed that even after the clearance of bacteria during the post-exposure treatment, the host succumbs to death due to the accumulation of toxin proteins in the host cells. While Abthrax, an anti-PA monoclonal antibody, is the only FDA-approved therapeutics used to treat post -exposure inhalational anthrax, again it causes severe irreversible tissue damage and death in the host. Vaccination is a prophylactic approach that can be utilized to control against the disease. Currently there are two different vaccine formulations against anthrax available on the market. They are the USA-licensed Biothrax (earlier known as Anthrax Vaccine Adsorbed (AVA)) and the UK -licensed Anthrax Vaccine Precipitate (AVP). Both of these vaccine formulations consist of *B. anthracis* cell-free culture supernatant, which is either adsorbed or precipitated with adjuvant aluminum hydroxide. However, these vaccines, being composed of the whole *B. anthracis* cell culture supernatant that are not free from the toxin counterparts, cause severe side effects.[7] To address these shortcomings, research is actively focused on subunit-based vaccines with full-length PA and its domains.[8,9] However, these vaccine candidates, unlike live/attenuated vaccines, are not efficiently immunogenic by themselves and require an adjuvant to increase their intrinsic immunogenicity.

Aluminum hydroxide (AH) has been the choice of adjuvant in vaccines since its first discovery in 1926 when Glenny and co-workers demonstrated the adjuvant potential of aluminum salts by mixing diphtheria toxin with alum.[10] AH adjuvant is USA FDA-approved for human use and has been used in hundreds of millions of doses in vaccines against Hepatitis A and B, tetanus, pertussis, diphtheria, and human papillomavirus with minimal side effects. AH adjuvants have been reported to elicit a robust Th2 response; however, they fail to induce a Th1 response, thus rendering them ineffective against intracellular pathogens like *Mycobacterium tuberculosis* (Mtb) and human immunodeficiency virus (HIV).[11] Although AH has been used as an adjuvant for a long time, consensus on the exact mechanism of its immunopotentiation has never been reached.

The physicochemical properties of aluminum salts, however, have been well characterized by Stanley Hem's group at Purdue University, and they have reported aluminum salts to be pseudo-crystalline and possess a boehmite-like structure with an average particle size of 2–8 μM. It has also been demonstrated that only 1.7% of the total surface area was available as an active site for vaccine antigen adsorption, while the rest of the sites might present within the colloidal particle itself.[12] Earlier studies on antigen adsorption and vaccine formulation showed that immune response relies on the amount of antigen that is adsorbed by the aluminum-containing adjuvant and not on the strength of adsorption. However, studies by Hansen et al.[13] on effect of the strength of adsorption of alpha casein to AH gel and phosphorylated AH gel on the immune response disclosed that the binding coefficient of the antigen to the AH adjuvant is a critical parameter for immune potentiation of the vaccine formulation.

In the present study, in an attempt to improve the adjuvant characteristics of traditional AH compounds, we have prepared crystalline and amorphous forms of AH nanoparticles (nps) with defined size and crystallinity. The biophysical and physicochemical properties of AH nps were evaluated by techniques like dynamic light scattering (DLS), X-ray diffraction (XRD), Fourier-transform infrared spectroscopy (FTIR), atomic absorption spectroscopy (AAS), Langmuir adsorption isotherm and isothermal titration calorimetry (ITC). The immunomodulating potential of AH nps was evaluated to ascertain if it can specifically impact the effect of APC activation and induce a better cellular immune response in comparison with the commercial adjuvant AH gel. Further, the protective efficacy of AH nps along with protective antigen domain 4 (D4) of *B. anthracis* against virulent anthrax spore challenge was evaluated in a mouse model.

Materials and Methods

Preparation of Amorphous and Crystalline AH nps

Amorphous and crystalline AH nps were prepared by varying the molar ratio of aluminum chloride and sodium hydroxide, according to the method described by Hsu et al.,[35] with slight modifications. Briefly, for the preparation of amorphous aluminum hydroxide nanoparticles (AH nps), equal volumes of 0.06 N $AlCl_3$ and 0.12 N NaOH were mixed by constant stirring and drop-wise addition of NaOH. For the preparation of crystalline AH nps, 0.06 N $AlCl_3$ and 0.18 N NaOH were mixed at equal volumes with continuous stirring. The cloudy precipitate was centrifuged and the pellet was washed with deionized water thrice before resuspending in phosphate buffer.

Characterization of Particles

The average population size of the prepared AH nps was measured by DLS. Samples were diluted in double distilled water and measured for size in a Malvern Zetasizer ZS90. Crystalline and amorphous characteristics of the prepared nanoparticles were analyzed using the XRD pattern of the lyophilized particles in PANalyticalX'pert PRO with a step size of 0.02º and counting time of 0.5 s per step over a 2θ range of 5º–70º. Aluminum content in the prepared AH nps suspension was estimated by AAS by comparing with a linear gradient of aluminium. FTIR spectra of the lyophilized AH nps were recorded in a Varian 7000 FTIR using the KBr pellet method and compared with the spectra of commercial AH gel.

Binding Efficiency of D4 to Amorphous and Crystalline AH nps

In order to determine the weight ratio at which D4 binds completely to amorphous and crystalline AH nps as well as AH gel, a binding assay was performed. Increasing amounts of D4 were mixed with a constant amount of the AH nps and incubated for 20 min at 4°C. Then the solution was centrifuged at 13,000 rpm and the unbound D4 present in supernatant was detected by SDS-PAGE.

FITC Labeling of Antigen D4

One milliliter of a 5 µg/µL stock of recombinant protein D4 was mixed with 100 µL of 1 mg/mL of FITC dissolved in DMSO and incubated for 4 h at room temperature with thorough mixing. Unbound FITC was separated by a G-25 sepharose column purification and D4-bound FITC was eluted by 1× PBS.

Cell Culture

The human monocytic cell line THP1 and mouse macrophage cell line RAW 264.7 used in this study were obtained from NCCS, Pune. RAW and THP-1 cells were cultured in Roswell Park Memorial Institute (RPMI) 1640 media supplemented with 10% FBS and maintained at 37°C in a humidified atmosphere with 5% CO_2. Prior to treatment, the monocytic THP1 cells were differentiated into macrophages with phorbolmyristate acetate (PMA) at a concentration of 20 ng/mL.

In-vitro Antigen Uptake Analysis

THP-1 cells at a cell density of 1 × 10^6/well were seeded onto 6-well tissue culture plates containing an autoclaved cover slip. After differentiating with PMA, media was replaced with fresh complete RPMI-1640 media and 20 µL of FITC-labeled D4 adsorbed onto AH nps or (AH gel) was added and incubated at 37°C and 5% CO_2 for 30 min. Unphagocytosed FITC were removed by washing the cells three times with PBS. Cells were fixed with 4% formaldehyde and washed twice with PBS. The cells containing cover slips were then mounted on to microscopic slides and viewed under a confocal microscope (Olympus FluoView FV1000).

Ethical Statement

All mouse experiments were performed in accordance with the relevant guidelines and regulations as approved by the Institutional Animal Ethics Committee, Central Laboratory Animal Resources, Jawaharlal Nehru University, New Delhi, India. Mice were housed in an individually ventilated animal caging system.

Immunologic Studies

Swiss albino mice were used throughout this study. The mice were immunized through the i.p. route with vaccines containing either the recombinant antigen D4 alone (20 µg/dose) or D4 adsorbed with amorphous or crystalline AH nps (50 µg/dose). Two subsequent booster immunizations were administered on days 14 and 28, with similar vaccine composition as in the primary dose. On days 14, 28 and 42, individual mice were bled via the retroorbital route. Plasma was separated by centrifugation and stored at –20ºC until use.

Evaluation of Total IgG and its Isotypes Antibody Titers

The antigen D4-specific presence of total IgG and isotypes IgG1 and IgG2-a antibody titers from the immunized mice sera was evaluated by enzyme-linked immunosorbent assay (ELISA) following the previously published method.[36] Briefly, 500 ng of purified recombinant protein D4 was coated in 96-well microtiter plates and incubated overnight at at 4°C. The next day, the protein solution was aspirated from the plate and washed twice with 1× PBS containing Tween-20 (0.05% v/v). The plate was blocked with 2% BSA for 1 h at 37ºC and then washed thrice with 1× PBS-T. Serial dilutions of the mice sera was added to the wells in triplicates and incubated for 2 h at 37ºC. The plate was then washed thrice with 1× PBS-T. The HRP conjugated secondary antibody (anti-mouse IgG-HRP) was added to the plates at a dilution of 1:10,000 and incubated for 1 h at 37ºC. After washing five times with 1× PBS-T, 100 µL of TMB substrate mixture was added to each well of the plate and incubated for 20 min in the dark for the color development. Then the reaction was stopped by adding 100 µL of 1N HCl prepared in water and absorbance noted immediately at 450 nm using a 96-well plate reader. For calculating the endpoint titers of antibodies, a cut-off value was first calculated from the sera of control mice group PBS and compared with test samples' absorbance. The cut-off is mean OD value plus three times standard deviation of the PBS control group in each respective dilution. Any sample dilution having absorbance higher than the cut-off value was considered a positive reading. The highest dilution and all the lower dilutions which had absorbance higher than the cut-off was chosen as the end point titer.

Isolation of Splenocytes and in-vitro Cytokine Release Measurement

Three weeks after the last immunization, three mice from each group were sacrificed and the spleens were aseptically removed. The spleen was homogenized in RPMI-1640 media using frosted slides and splenocytes were separated using a 90-µm nylon mesh filter. The red blood cells were lysed using 0.9% ammonium chloride solution. The final cell pellet was washed once with incomplete RPMI-1640 media and suspended in complete RPMI-1640 media supplemented with 10% fetal bovine serum. The cells were then plated at a cell density of 1×10^5 cells/well in 96-well tissue culture plates and stimulated with 5 µg/mL ConA (positive inducer), 5 µg/mL D4 (test) or media only (negative control) in triplicate. Culture supernatants were collected after 72 h of incubation and cytokine levels were evaluated using an opt-EIA kit (BD Biosciences Pharmigen, San Diego, CA) as per the manufacturer's instructions.

Toxin Neutralization Assay

The protective efficacy of the antibody against the anthrax toxin was determined as a measure of the capacity to protect the RAW 264.7 cell line, a murine macrophage cell line from lethal toxin (LeTx). Briefly, RAW 264.7 cells (1×10^4 cells/well) were seeded in 96-well flat-bottom tissue culture plates. Anti-D4 IgG dilutions (in incomplete RPMI 1640) were added and mixed with EC_{50} of lethal toxin (500 ng/mL PA and 1 µg/mL LF) for 1 h at room temperature. One hundred microliters of this complex were added to the cells and incubated for 4 h. In order to find the cell viability, 100 µL of MTT (0.5 mg/mL; prepared in incomplete RPMI 1640 media) was added to each well and incubated for 30 min. One hundred microliters of DMSO were added to solubilize the formazan crystals and the absorbance was noted at 540 nm. Cells treated with only media were taken as a control.

Anthrax Spore Challenge

For the anthrax spore challenge, each mouse group (n= 10), immunized with PBS or D4 only or D4 + amorphous AH nps or D4 + crystalline AH nps or D4 + AH gel, were challenged with 0.5×10^3 spores of a clinical virulent strain of BA via the i.p. route after 45 days of primary immunization. Infected mice were kept in isolator in BSL3 and observed for 14 days for death and morbidity. Percentage survival of the vaccine formulations was compared and represented by plotting a Kaplan–Meir curve.

Thermodynamics and Kinetics of D4–Adjuvant Interaction and Release Profile

Langmuir Adsorption Isotherm

The binding isotherms of D4 with both amorphous and crystalline aluminum hydroxide nanoparticles were performed to estimate the binding capacity and adsorption coefficient.[13,37] The Langmuir equation[15] may be described as adsorption of solute onto the surface in a monolayer. Briefly, protein working solutions were prepared at a concentration twice that of the final desired concentration. An equal volume (0.5 mL) of protein working solution and adjuvant suspensions (100 µg/mL) in 0.1 M phosphate

buffer, pH 7.4, were combined in 1.5-mL centrifuge tubes. The suspensions were gently mixed by end to end rotation at 4°C for 30 min. The amount of protein adsorbed was calculated by centrifuging the samples at 10,000 rpm and analyzing the supernatant by the micro-BCA method. The amount of protein adsorbed was calculated by subtracting the protein unadsorbed from the protein initially added.

Isothermal Titration Calorimetry

ITC measurements were performed to measure the binding of D4 with amorphous and crystalline AH nps as well as AH gel at 25°C on a MicroCal iTC200 (Malvern Instruments Ltd, UK). All proteins and adjuvants were dissolved in the gently degassed 0.1 mM phosphate buffer, pH 7.4. A total volume of 40 µL from the injection syringe was added to a sample cell containing 280 µL of adjuvant. A total of 20 injections with each injection of 2 µL of D4 was titrated into the sample cell containing 500 µg/mL of either amorphous, crystalline AH nps or aluminum hydroxide gel simultaneously and each injection was separated by 150-s intervals to allow the signal to return to baseline. A constant stirring speed of 300 rpm was maintained to ensure proper mixing after each injection. Control experiments were performed under similar conditions by titrating proteins into buffer and were subtracted to correct the heat of ligand dilution. Thermodynamic parameters were obtained by fitting the corrected data to a non-competitive one sets of sites model using origin software.

In-vitro Antigen Release Assay

In order to know the plausible release profile of antigen D4 from AH nps at the injection site after immunization in mice, the in-vitro antigen release assay was performed by following the method published previously.[36,38] Briefly, 250 µg of D4 were incubated with 500 µg of the prepared AH nps adjuvants for 20 min. This formulation was mixed with 1× PBS at a ratio of 1:3 to form a stock solution and incubated at 37°C with 80 rpm shaking speed. Samples were collected at different time intervals for the next week, centrifuged and the supernatant collected. The amount of protein released in the supernatant was estimated by the micro-BCA method (Thermo Scientific Micro BCA kit) as per the manufacturer's protocol.

Statistical Analysis

For the physicochemical experiments, the data were prepared and analyzed by using either Sigma Plot or Microsoft excel. For mouse immunological studies, GraphPad Prism v6.05 software was used for data preparation and statistical analysis. To calculate the significance of difference between vaccinated mice groups, either one-way or two-way ANOVA followed by Tukey's multiple comparison tests were employed. A P value <0.05 was considered as significant, * <0.05, **<0.01, ***<0.001, ****<0.0001. ns, non-significant.

Results

Biophysical Characterization of Crystalline and Amorphous AH nps in Comparison with Commercial AH Gel

The average population size of the amorphous and crystalline AH nps were determined by DLS analysis and were found to be 230 nm and 180 nm, respectively (Figure 1A). As shown in XRD analysis, the presence of broad-hump spectra with no sharp diffraction peaks in Figure 1B and a sharp diffraction peak in Figure 1C confirm the amorphous and crystalline characteristics of the prepared AH nps. As expected, the XRD analysis of commercial adjuvant AH gel showed several broad-hump spectra (Figure 1D). The aluminum content present in the prepared crystalline and amorphous AH nps suspensions was determined by AAS and was calculated to be 504 µg/mL and 510 µg/ml, respectively. Further, the surface composition characterization of the prepared AH nps was performed by FTIR analysis (Figure 1E) in comparison with the commercial AH gel at 400–4000 cm^{-1} spectral range. The bands at 3000–3700 cm^{-1}in the prepared AH nps shows the (Al)O–H stretch, while the bands at 1080 cm^{-1} show that aluminum (Al) is hydrated, i.e. Al–(OH) bond formation. Consistent with the XRD data, the FTIR results reaffirmed the formation of amorphous and crystalline-like AH nps. Further, the antigen-adjuvant binding assay was performed in order to find out the weight ratio at which D4 binds completely to the AH nps. From the results (Figure 1F) it was observed that antigen D4 binds completely to both amorphous and crystalline AH nps at a weight ratio of 1:1 of adjuvant and antigen complex, while AH gel is able to adsorb the antigen D4 at a weight ratio of 2:1, which shows the presence of a larger surface area in crystalline and amorphous AH nps for antigen binding than that of AH gel.

Crystalline and Amorphous AH nps Showed Enhanced Antigen D4 Uptake in THP-1 macrophages

Due to their size, nanoparticles showed increased cellular uptake by APCs than that of microparticles in some of the

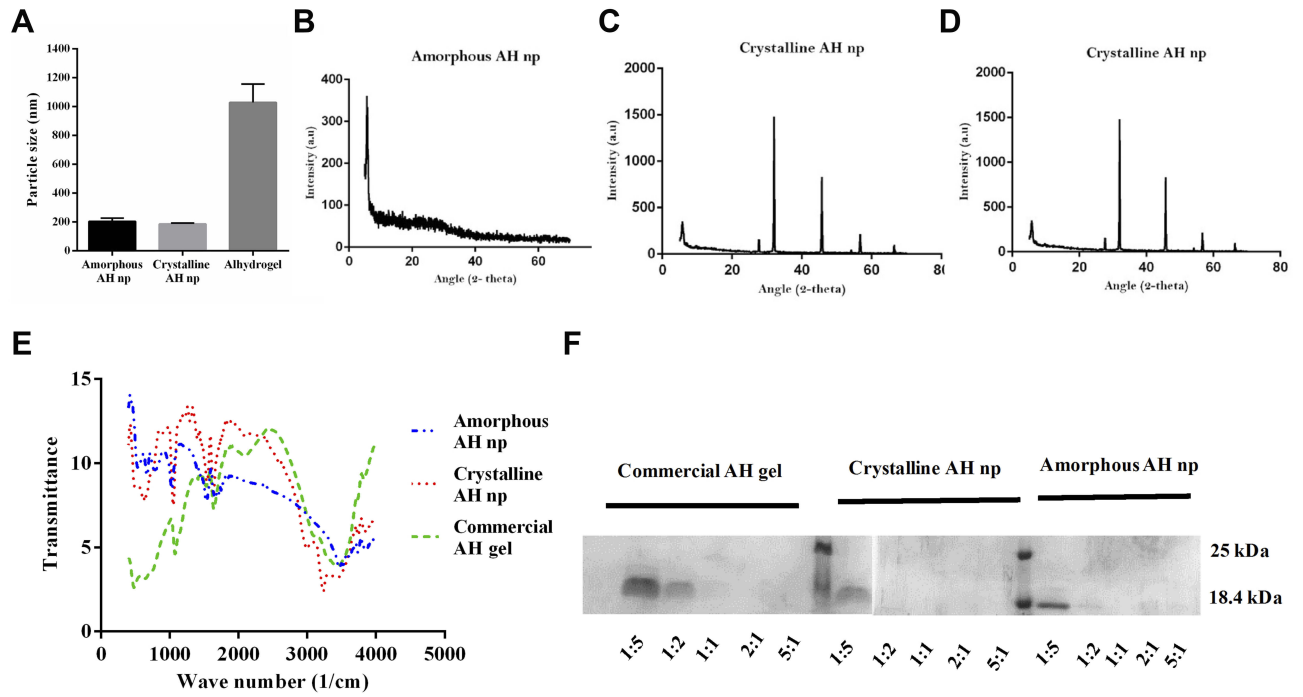

Figure 1 Physical characterization of amorphous and crystalline AH nps in comparison with commercial adjuvant AH gel. The average population size of the nanoparticles was measured by DLS in a Malvern Zetasizer ZS90 (**A**). Crystallinity of the prepared nanoparticles was analyzed using the XRD pattern of the lyophilized particles in PANalytical X'pert PRO. Comparative XRD analysis of amorphous AH nps (**B**), crystalline AH nps (**C**) and AH gel (**D**). FTIR spectrographs of amorphous AH nps, crystalline AH nps and AH gel (**E**). Binding of D4 with amorphous AH nps, crystalline AH nps and AH gel at different weight ratio of adjuvant. Varying weight of D4 was incubated with a constant weight of the adjuvant. Post-incubation, the samples were centrifuged and unbound D4 analyzed in the supernatant by SDS-PAGE (**F**).

recently reported studies. Thus, in the present study, the intracellular uptake of the AH nps prepared in this study by THP-1 macrophage cells were evaluated in comparison with commercial AH gel. The antigen D4 used for this study was first conjugated with fluorescent dye (FITC) and then adsorbed onto the AH nps surface before the cellular treatment. The uptake of both amorphous and crystalline AH nps as well as AH gel adsorbed with FITC-labeled antigen D4 was seen under confocal microscopy. From the results (Figure 2), it was observed that both amorphous and crystalline AH nps showed increased phagocytosis of antigen D4 as compared to the AH gel group, which is in agreement with previous studies.[14]

Crystalline and Amorphous AH nps Elicited Enhanced Antigen D4-Specific Humoral Immune Response

In order to evaluate the ability of crystalline and amorphous AH nps in modulating the antigen D4-specific immune response, the mice were immunized with crystalline and amorphous AH nps adsorbed with antigen D4 three times with 2-week intervals between each immunization. Group of mice were immunized with the commercial adjuvant AH gel along with antigen D4 to serve as a positive control. After two weeks of each immunization, blood sera were collected from the immunized mice and the presence of antigen D4-specific total IgG and isotypes (IgG1 and IgG2-a) antibody titers was measured by indirect ELISA.

Both the crystalline and amorphous forms of AH nps enhanced the levels of antigen D4-specific total IgG antibody titers starting from day 14 as compared to the antigen D4 alone group (Figure 3A). However, a significant difference in the enhancement of total IgG was observed only on days 28 and 42 crystalline and amorphous AH nps group than the D4-only group (Figure 3A). The increase observed from the crystalline and amorphous AH nps groups were also significantly higher than that of AH gel group ($P \leq 0.0001$) at day 42. As compared between the amorphous and crystalline AH nps groups, the levels of total IgG titers significantly higher in the crystalline AH nps ($P \leq 0.01$). In order to know the nature of the immune response induced by crystalline and amorphous AH nps, the presence of antigen D4-specific Th2-type IgG1 and Th1-type IgG2-antibody isotypes from the immunized mice sera were evaluated. The levels of IgG1 titer were similar between the amorphous AH nps and AH gel mice

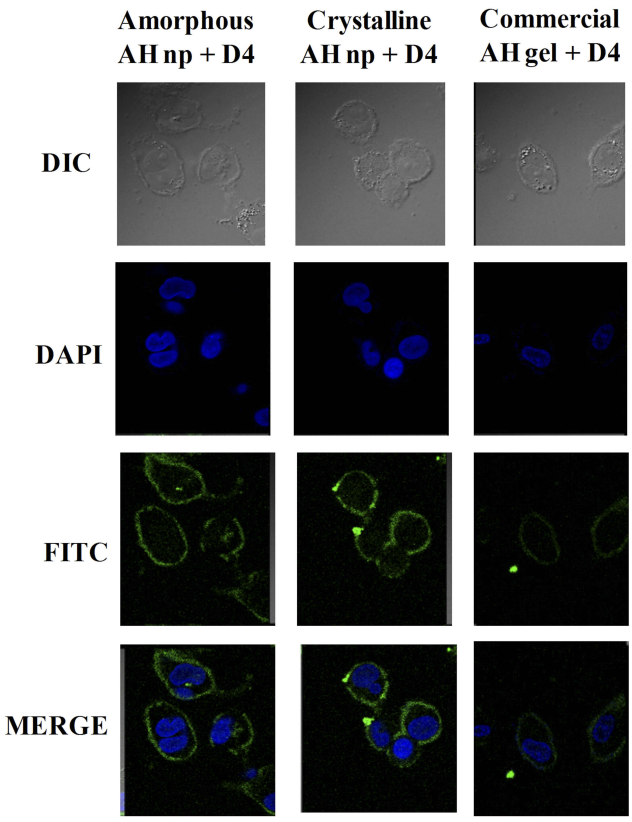

Figure 2 In-vitro uptake efficiency of FITC-labeled antigen D4 adsorbed on amorphous and crystalline AH nps by THP1 macrophages. Confocal microscopic images of THP1 macrophages incubated with amorphous AH nps, crystalline AH nps and AH gel adsorbed with FITC-D4 for 30 min at 37°C in 5% CO_2.

groups, while crystalline AH nps level was significantly higher ($P \leq 0.01$) than the AH gel group (Figure 3B). The levels of IgG2-a titers were significantly higher in both the crystalline and amorphous AH nps than the AH gel group (Figure 3C). When compared between the crystalline and amorphous AH nps, the levels of IgG1 were similar, whereas the levels of IgG2-a were significantly higher in the crystalline AH nps ($P \leq 0.01$).

Crystalline and Amorphous AH nps Elicited a Mixed Th1 and Th2 Cell-Mediated Immune Responses

Previous reports suggest that a mixed T-helper (Th) immune response is favorable to combat anthrax infection. Th cells (Th1/Th2) play important roles in mediating both humoral and cellular responses via the expansion of antigen-stimulated B cells and $CD4^+$ Th cells. The cytokines IL-2 and IFN-γ are predominantly produced by activated Th cells involved in activation of T-helper 1 (Th1) immune responses while cytokines IL-4 and IL-10 are mainly produced by T-helper 2 (Th2) cells involved in promotion of the Th2-type immune response. In order to see further the ability of amorphous and crystalline AH nps on inducing antigen D4-specific cell-mediated immunity, the release of antigen D4-specific Th1 (IL-2 and IFN-γ) and Th2 (IL-4 and IL-10) type cytokines in the culture supernatant of in-vitro stimulated splenocytes was measured. As shown in Figure 4, the mice groups immunized with PBS and antigen D4 only produced low quantities of all four cytokines in response to antigen D4. As expected, the AH gel mice group induced exclusively Th2-type cytokines IL-4 and IL-10 (Figure 3B and C). Conversely, the D4 adjuvated with amorphous and

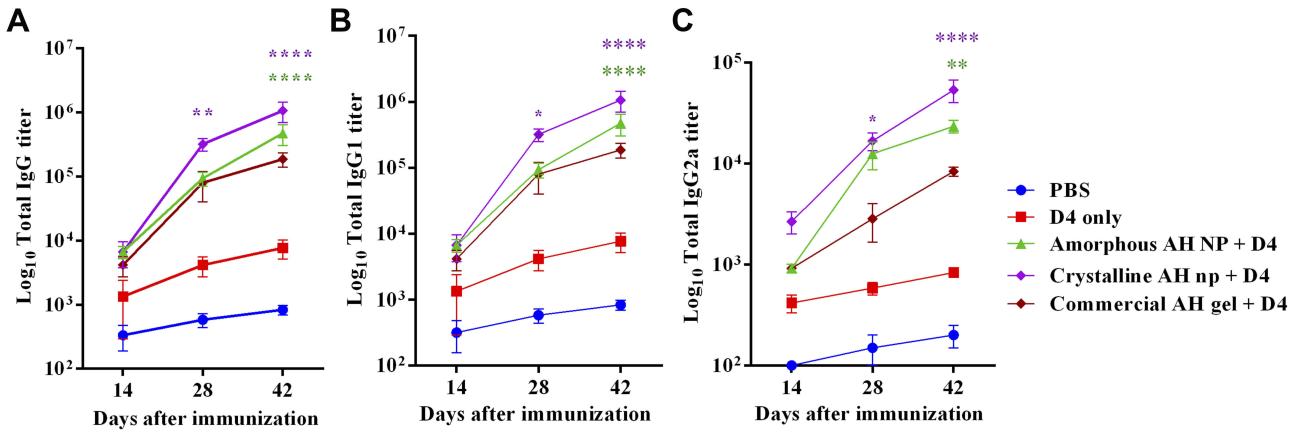

Figure 3 Antigen D4-specific humoral immune response induced by vaccination with amorphous and crystalline AH nps. Mice were immunized either with the antigen D4 alone or adsorbed onto amorphous or crystalline AH nps or with control adjuvant AH gel three times with a two-week interval between immunization via the i.p. route. Two weeks after the last immunization, sera was collected from the individual immunized mice (n= 5) from each immunized mice groups. The presence of antigen D4-specific total IgG (**A**), and isotypes IgG1 (**B**) and IgG2a (**C**) titers was measured by ELISA. The results were expressed as mean value with standard error of mean of between mice in a single mice group. *P* value was calculated between vaccinated mice groups using two-Way ANOVA followed by Tukey's multiple comparison test. *P < 0.05, **P< 0.01, ****P < 0.0001. n.s., non-significant.

crystalline AH nps groups showed elevated levels of both Th1 and Th2 cytokines. In comparison, the levels of Th2 cytokines IL-4 and IL-10 were significantly higher in the AH gel group ($P< 0.01$ for IL-4 and $P< 0.0001$ for IL-10) than the AH nps group. The levels of Th1 cytokines IFN-γ and IL-2 was remarkably higher in the crystalline and amorphous AH nps group ($P < 0.0001$) than the AH gel group (Figure 4A and D). Moreover, the comparison between amorphous and crystalline AH nps groups showed that the levels of Th1-type IFN-γ and Th2-type IL-4 and IL-10 cytokines were statistically indifferent between the two groups, whereas production of Th1-type IL-2 cytokine was significantly higher in the crystalline AH nps group ($P< 0.05$) (Figure 4). In addition to Th1 and Th2 cytokines, the inflammatory response -specific cytokine IL-1β were also measured from the in-vitro stimulated splenocytes culture supernatant. The result displayed that the levels of IL-1β cytokine in the crystalline and amorphous AH nps group was significantly higher than the AH gel group (Figure 4E).

Crystalline and Amorphous AH nps Immunized Mice Sera Effectively Neutralized LeTx Toxin and Protects RAW264.7 Cells

A toxin neutralization assay (TNA) assay was performed in order to evaluate the LeTx toxin-neutralizing potential of the anti-D4 antibodies present in the sera of mice immunized with crystalline and amorphous AH nps with antigen D4 and whether the RAW264.7 cells were protected from the toxin. The in-vitro TNA was performed by incubating RAW264.7 cells with either the LeTx toxin alone or LeTx pre-incubated with serially diluted anti-D4 sera. The results showed that the cells incubated with the toxin LeTx pre-incubated with control group PBS mice sera were not able to protect the RAW264.7 cells from LeTx toxin-mediated killings (Figure 5A). In contrast, the crystalline and amorphous AH nps sera were able to neutralize the LeTx toxin effectively and provided up to 90% protection, while AH gel sera was able to provide up to 75% protection.

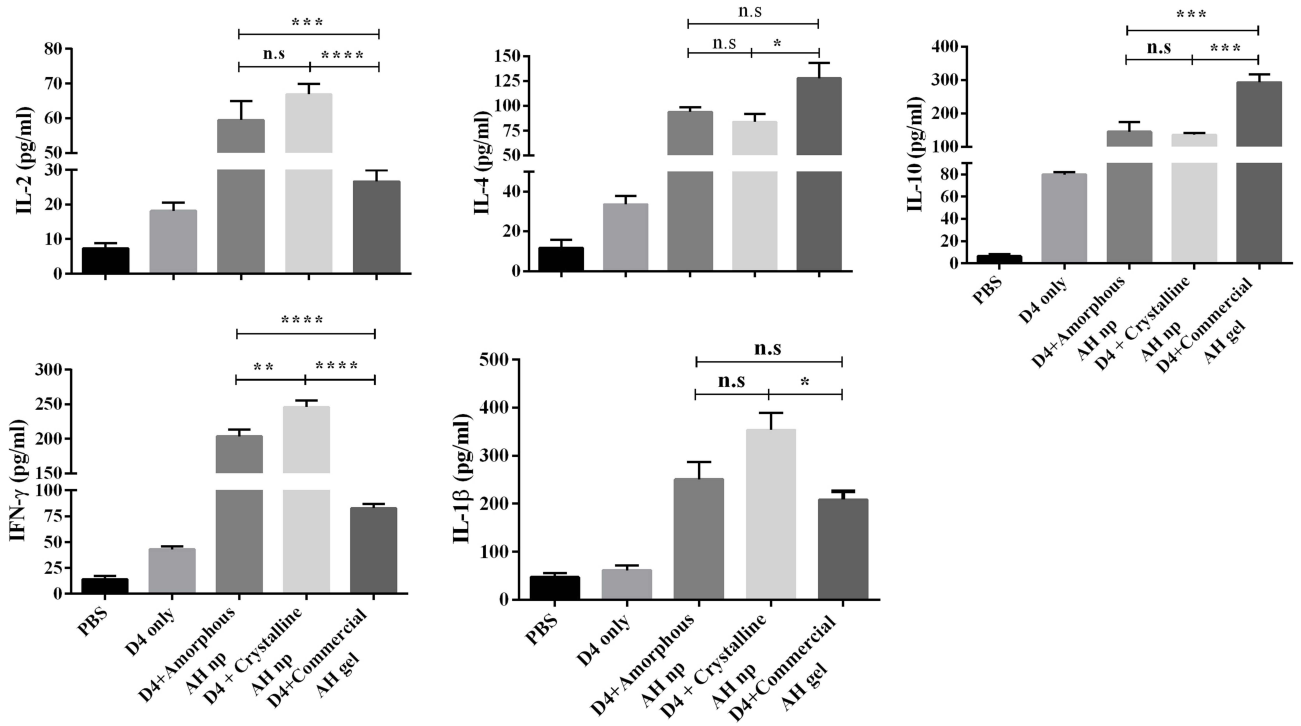

Figure 4 Antigen D4-specific cellular immune response induced by vaccination with amorphous and crystalline AH nps. Mice were immunized either with the antigen D4 alone or adsorbed onto amorphous or crystalline AH nps or with control adjuvant AH gel three times with a two-week interval between immunization via the i.p. route. Three weeks after the last immunization, splenocytes were isolated from individual mice (n= 5) in each group, cultured in an in-vitro condition in the presence of antigen D4 for 72 h at 37°C with 5% CO_2. The release of antigen D4-specific Th1-type IL-2 (**A**), IFN-γ (**D**), Th2-type IL-4 (**B**) and IL-10 (**C**) and inflammasome-specific IL-1β (**E**) cytokines were measured from the culture supernatant by ELISA using an opt-EIA kit. The results were expressed as mean value with standard error of mean of between mice in a single mice group. *P* value was calculated between AH nps adjuvanted and AH gel groups using one-way ANOVA followed by Tukey's multiple comparison test. *P < 0.05, **P< 0.01, ***P< 0.001, ****P < 0.0001. n.s., non-significant.

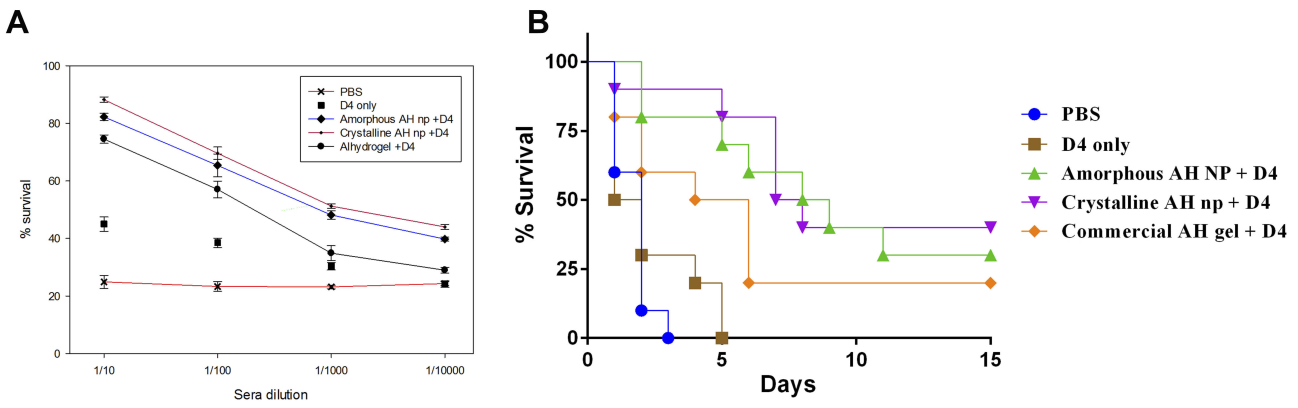

Figure 5 Toxin neutralization and protective efficacy analysis of the antigen D4 vaccination with amorphous and crystalline AH nps. Lethal toxin neutralization assay was performed with anti-D4 sera dilutions of mice groups immunized with either the antigen D4 alone or with amorphous or crystalline AH nps or AH gel. Serial dilutions of sera were mixed with lethal toxin (500 ng/mL PA and 1 μg/mL LF) and incubated with RAW 264.7 cells at 37°C and 5% CO_2 for 4h. The cell viability was measured by MTT assay. Cells without toxin treatment were taken as negative control and their absorbance was used as 100% viability (**A**). Protective efficacy of the vaccine formulations against *B. anthracis* spore challenge was evaluated in Swiss albino mice. Fourteen days after the second booster, mice were administered with 0.5×10^3 spores of a virulent strain of *B. anthracis*. Infected mice were kept in an animal isolator in BSL3 and observed for death and morbidity for 14 days (**B**). The toxin neutralization assay was performed from pooled sera of a single group (n= 5) in triplicate and expressed as mean value with standard deviation (SD).

Crystalline and Amorphous AH nps Provides Superior Protection Against Anthrax Spore Challenge as Compared to AH Gel

The protective efficacy of the vaccine formulations was evaluated against anthrax spore challenge after day 45 of prime immunization. Both vaccinated as well as non-vaccinated mice groups were infected with 0.5×10^3 spores of a virulent strain of *B. anthracis* and observed for death and morbidity for the next 14 days. The control mice group vaccinated with PBS and antigen D4 only could not provide protection against the spore challenge and all the mice succumbed to death within 3–5 days of infection (Figure 5B). Although the antigen D4 adjuvanted with AH gel group was able to offer 20% protection against the anthrax spore challenge, a significant increase in the mean time to death (MTD) was observed in the mice groups immunized with amorphous and crystalline AH nps with D4 enhanced the protection up to 30% and 40%, respectively.

Crystalline and Amorphous AH nps Showed Enhanced Antigen Binding and Release

In order to probe the difference in the immune response observed from the crystalline and amorphous AH nps as well as from AH gel, thermodynamic studies of D4 binding affinity to the AH nps were carried out by performing Langmuir adsorption isotherm (Figure 6A) and ITC (Figure 7A and B). The amount of antigen D4 adsorbed onto the crystalline and amorphous AH nps and the strength of binding affinity present between antigen D4 and the AH nps was determined by constructing adsorption isotherms. The adsorptive capacity of crystalline and amorphous AH nps with antigen D4 was performed at pH 7.4 to determine the binding capacity (amount of protein adsorbed at a monolayer coverage) and adsorptive coefficient (which is the measure of the affinity of the protein towards the adjuvant surface).[15] On linearizing the adsorption isotherm, the adsorptive capacity of crystalline and amorphous AH nps with D4 was calculated to be 1.65 and 1.81 μg/μg, respectively (Figure 6B). Titration of D4 with amorphous AH nps (Figure 7A) gave rise to endothermic peaks with a gradual decrease with the progress in the reaction depicting a decrease in free surface area for binding. In contrast, titration of D4 with crystalline AH nps (Figure 7B) was exothermic in nature. The binding constant obtained from ITC data was roughly similar to the adsorption coefficient value obtained from the adsorption isotherm and was determined to be 8.9 e4 and 4.6 e4, respectively, for amorphous and crystalline AH nps. From the binding enthalpy and entropy data, it was also observed that the binding between D4 and the adjuvants were entropically driven but were enthalpically unfavorable (Figure 7C).

The release kinetics of D4 from the crystalline and amorphous AH nps were studied by in-vitro release assay. Samples were drawn at different time intervals for one week and D4 release was quantified in the supernatant by the micro-BCA

A

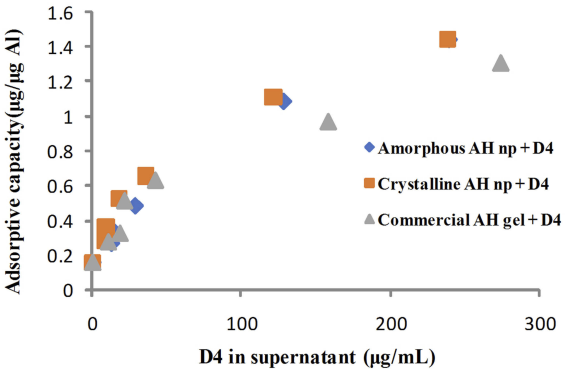

B

Adjuvant	Adsorptive capacity (µg /µg Al)
Amorphous AH np	1.81
Crystalline AH np	1.65
Commercial AH gel	1.49

Figure 6 Langmuir adsorption isotherm for surface area measurement for antigen binding onto amorphous and crystalline AH nps: an increasing amount of D4 was incubated with a constant amount of either amorphous AH nps or crystalline AH nps or AH gel for 20 min. Post-incubation, the samples were centrifuged and the presence of D4 in the supernatant was analyzed by micro-BCA assay. The amount of D4 adsorbed onto the adjuvants was calculated by subtracting the amount of D4 added initially in the solution. The adsorptive capacity was obtained by linearizing the adsorption isotherm. The graph shows the comparative binding of D4 onto amorphous AH nps, crystalline AH nps as compared to AH gel (**A**). The table shows the linearized adsorption isotherm curves for calculating the values for adsorptive capacity (**B**).

A

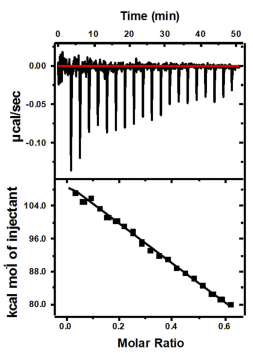

B

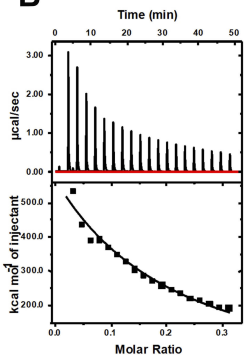

C

D4 (60 µM)	K_a (M^{-1})	ΔH (Kcal/mol)	ΔS (Kcal/mol/deg)
Amorphous AH np	8.9e4	2398e3	8040
Crystalline AH np	4.6e4	164	0.57
Commercial AH gel	9.23e4	2989e3	0.033

D

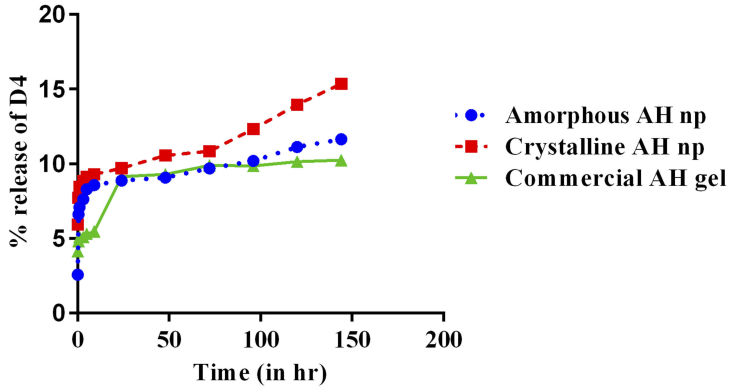

Figure 7 Binding energetics and in-vitro release kinetics of antigen D4 from amorphous and crystalline AH nps. D4 was titrated against the adjuvants with constant stirring at room temperature. Thermodynamic parameters were obtained by fitting the corrected data to a non-competitive set of sites model using origin software. The results show the thermograms of titration of D4 with amorphous AH nps (**A**) and crystalline AH nps (**B**). Table shows the values of comparative thermodynamics data of titration of D4 with amorphous AH nps and crystalline AH nps in comparison to AH gel (**C**). Release kinetics of D4 from amorphous AH nps, crystalline AH nps and AH gel was compared from the in-vitro release assay (**D**).

method. As depicted in Figure 7D, it was observed that D4 follows very-slow-release kinetics from the AH nps. The rate of elution of D4 was observed to be slow in amorphous AH nps followed by crystalline AH nps and AH gel.

Discussion

Both AVA and AVP, the two licensed human vaccines against anthrax, contain aluminum hydroxide salts as adjuvants. However, these vaccines require a cumbersome

dosing schedule to elicit correct protective antibodies against the disease. The development of improved vaccine candidates against anthrax has been pursued for a long time with studies like polylactic-co-glycolic acid (PLGA) encapsulated D4 nanoparticles,[6] and PLGA-dendron nanoparticle-based PA-DNA vaccine,[16] dual-function viral nanoparticle,[17] CpG-Ficoll nanoparticle adjuvant encapsulating PA,[18] and Tri-methyl chitosan nanoparticles containing PA,[19] where the authors have shown induction of a better immune response and disease protection as compared to the traditional anthrax vaccines. Moreover, alum, being a Th2-type adjuvant, fails to clear the intracellular pathogens, thus rendering the vaccines ineffective in certain diseases like tuberculosis.[11] Despite many adjuvants being developed for human use, alum- and aluminum salt-based adjuvants still continue to be the choice for human use, due to its non-toxic and safety profiles. The recent advancement in the field of nanotechnology has also paved the way for developing new nanoparticle-based adjuvants with controlled size, shape and surface properties in order to obtain the desired immune response for a particular type of disease. Nanoparticles offer the advantage of dose sparring, controlled antigen release, shaping the antibody response toward the functionally desired type, eliciting a rapid immune response, and providing a long -lasting memory response.[20,21] Although studies have reported microparticles to be efficiently phagocytosed by macrophages, the works of Kanchan et al. and Fifis et al.[22,23] have demonstrated that particles ranging from 200 to 600 nm show enhanced phagocytosis and induce a strong antigen-specific humoral and cellular immune response. Previous studies on modified nanoscale preparation of the alum components have been shown to have potential advantages over the traditional form of alhydrogel.[14,24–26] Recently it was shown by Orr et al.[27] that stable nanoparticle preparation from the conventional adjuvant alhydrogel by including a poly(acrylic acid) (PAA) polymer elicited a more robust antigen-specific Th1 immune response than alhydrogel.[27]

In an attempt to improve the adjuvant characteristics of traditional aluminum hydroxide compounds, in the present study, we have prepared crystalline and amorphous forms of AH nps and evaluated its physicochemical and immunomodulating potential by utilizing antigen D4 of *Bacillus anthracis*. APCs play crucial roles in antigen recognition, processing and presentation along with either MHC class I or II molecules to the other immune cells, e.g. T-helper (Th) and T-cytotoxic (Tc) cells, which in turn establish strong antigen-specific adaptive immune response in the host. From the in-vitro results it was observed that crystalline and amorphous AH nps adsorbed with FITC-labeled antigen D4 are efficiently taken up by THP-1 macrophages as compared to the AH gel microparticles (Figure 2). It is likely that the nanometer range size of the particles facilitated the efficient uptake of antigen D4 by THP-1 macrophages through phagocytosis.[14] It is known that aluminum salt-based adjuvants majorly induce Th2-biased immune response possibly due to their immunosuppressive effect on the Th1 immune response as well as decreased cross-presentation of the adsorbed antigen,[13] prohibiting its use against intracellular pathogens like Mtb, where the Th1 immune response has been shown to be critical for disease resistance.[28] Our study results are in agreement with previous findings that AH gel exclusively induced Th2-biased immune response (Figures 3B, 4B and 4C).[29] In contrast, the crystalline and amorphous forms of AH nps prepared in this study induced statistically higher Th1-type cytokines IL-2 ($P< 0.001$ and $P< 0.0001$ for amorphous and crystalline AH nps) and IFN- γ ($P< 0.0001$ and $P< 0.0001$ for amorphous and crystalline AH nps) in immunized mice as compared to the AH gel group, indicating an effective presentation of the antigen with MHC class II molecules by APCs to the Th cells. Moreover, the increased production of IL-2, known to be important for promoting the development of naïve $CD4^+$ Th cells to effector and memory $CD4^+$ Th cells, and IFN-γ predominantly produced $CD4^+$ Th cells and $CD8^+$ Tc effectors cells, are a good indication of inducing a Th1 immune response in the AH nps mice groups. Previously, Mori et al.[30] reported that the induction of a Th1 immune-specific response to IL-12 cytokine by dendritic cells (DCs) was blocked through the inhibition of IL-12p35 transcription factor in the alhydrogel-adjuvanted mice. Additionally, it has been demonstrated recently that alum adjuvant activates immunosuppressive mechanisms following vaccination with the help of increased production of IL-10 cytokine by macrophages and DCs, which limits its ability to induce Th1-type immune responses.[31] As observed in this study, the level of IL-10 cytokine in both AH nps immunized mice groups was statistically low as compared to the commercial adjuvant AH gel group ($P< 0.001$). Taken together with the results of enhanced productions of Th1-type cytokines, the decreased production of IL-10 cytokine indicates that the induction of Th1-type immune response in the crystalline and amorphous AH nps mice groups were not restrained.

NLRP3 (nucleotide-binding domain leucine-rich repeat-containing protein) receptor dependent inflammasome activation and increased production of IL-1β cytokine is another way

alum-based adjuvants mediate their adjuvant function.[32] The levels of IL-1β cytokine in the crystalline and amorphous AH nps-adjuvanted groups were significantly higher in comparison to the AH gel group, which indirectly indicates that these AH nps have higher effect on NLRP3 inflammasome activation (Figure 4E). Based on the antigen D4 uptake with crystalline and amorphous AH nps by THP-1 cells results, it can be concluded that the nanoscale size of the particles might have helped the APCs to uptake antigen D4 more efficiently than the AH gel group, which resulted an increased inflammatory response and high level of IL-1β secretion.[13] Also, alum causes cell death and the release of numerous molecules, e.g. uric acid and ATP from the damaged cells that accumulate at the sites of alum injection and act as damage-associated molecular patterns (DAMPs). The molecule ATP potentiates its inflammasome activation via binding to the cellular P2X purinoceptor (P2X7) receptor while uric acids inflammasome activation is shown to be dependent on the interleukin-1 receptor (IL-1R) and downstream myeloid differentiation molecule 88 (MyD88) signaling pathway. Further, the release of uric acid and ATP molecules stimulates dendritic cells to mature, the expression of various cellular co-stimulatory molecules and augments the priming of $CD8^+$ T-cell responses to the cross-presented antigen.[33,34]

Another mechanism by which alum-based adjuvants mediate its function is by retaining the antigen at the injection site and releasing it over an extended period of time. The antigen retention by aluminum salts results in a high concentration of antigens at the site of injection which helps recruitment of a large number of inflammatory cells and APCs to the injection site, effectively interacting with antigens and reinforcing the strong immune response. Studies by Hansen et al.[13] have reported that the binding strength present between the antigen and adjuvant interaction is a crucial parameter for slower antigen release and strengthened immune response. However, extremely strong adsorption of the antigen may interfere with the immune response at least in part by interfering with antigen processing in APCs.[13] The binding affinity strength analysis of antigen D4 with crystalline and amorphous AH nps (Figure 7C) revealed that amorphous AH nps hold stronger antigen binding than the crystalline AH nps which resulted in a lesser immune response than the crystalline AH nps group. These results matched well with the in-vitro antigen release study, where it was seen that D4 is released more slowly from amorphous AH nps than crystalline AH nps. Hence, the varied immune response observed between amorphous and crystalline AH nps can be attributed to the strength of binding affinity of the antigen, which is in agreement with the study conducted by Hansen et al.

In conclusion, we have designed and prepared two different AH nps with defined size and crystallinity and evaluated their physiochemical and immune-stimulating properties in comparison with commercially available adjuvant AH gel. The results demonstrate that the physical attributes of the adjuvant can be engineered in such a way as to modulate the adaptive immune system. Not only did these AH nps boost the antigen D4-specific antibody titer, they activated a strong Th1 -mediated immunity with increased inflammation activation as compared to the commercial adjuvant AH gel. The increased immune response observed with AH nps can possibly be attributed to the enhanced antigen uptake, processing and presentation to the Th cells by APCs. Moreover, the D4 adjuvanted with AH nps immunized mice group showed superior protection against anthrax spore challenge in comparison to the AH gel group. The comparative physicochemical studies revealed a moderate binding affinity of crystalline AH nps with antigen D4 than its counterpart amorphous AH nps and resulted in moderate antigen release. Altogether, the strong Th2 and Th1 immune response induced by AH nps signifies that nanoparticle-based alum adjuvant can be a potential alternative over microparticle-based AH gel adjuvant in the near future. Additionally, this type of AH nps can be a better choice of adjuvant for vaccines where Th1 immunity is a major concern. However, further studies to evaluate the adjuvant potential of AH nps against intracellular pathogens like Mtb and deciphering the mechanism on how AH nps potentiate its antigen-specific Th1 immune response will be a key for the successful development of AH nps-based vaccine candidates.

Acknowledgments

We would like to thank Advanced Instrumentation Facility (AIRF), Jawaharlal Nehru University (JNU) and Shriram Institute for Industrial Research for the technical assistance with FTIR, XRD, AAS and confocal microscopy. We would also like to thank Department of Biotechnology Government of India for providing financial assistance for BSL-3 facility operation and maintenance.

Disclosure

The authors declare that the research was conducted in the absence of any commercial/financial or non-financial relationships that could be construed as a potential conflict of interest and that they have no conflicts of interest in this work.

References

1. Dixon TC, Meselson M, Guillemin J, Hanna PC. Anthrax. *N Engl J Med*. 1999;341(11):815–826. doi:10.1056/NEJM199909093411107
2. Greenfield RA, Bronze MS. Prevention and treatment of bacterial diseases caused by bacterial bioterrorism threat agents. *Drug Discov Today*. 2003;8(19):881–888. doi:10.1016/S1359-6446(03)02847-2
3. Ibrahim KH, Brown G, Wright DH, Rotschafer JC. Bacillus anthracis: medical issues of biologic warfare. *Pharmacotherapy*. 1999;19(6):690–701. doi:10.1592/phco.19.9.690.31543
4. Leppla SH. Anthrax toxin edema factor: a bacterial adenylate cyclase that increases cyclic AMP concentrations of eukaryotic cells. *Proc Nat Acad Sci*. 1982;79(10):3162–3166. doi:10.1073/pnas.79.10.3162
5. Mock M, Fouet A. Anthrax. *Ann Rev Microbiol*. 2001;55(1):647–671. doi:10.1146/annurev.micro.55.1.647
6. Manish M, Rahi A, Kaur M, Bhatnagar R, Singh S. A single-dose PLGA encapsulated protective antigen domain 4 nanoformulation protects mice against Bacillus anthracis spore challenge. *PLoS ONE*. 2013;8(4):e61885. doi:10.1371/journal.pone.0061885
7. Peakman M, Skowera A, Hotopf M. Immunological dysfunction, vaccination and Gulf War illness. *Philos Trans R Soc B*. 2006;361(1468):681–687. doi:10.1098/rstb.2006.1826
8. Chauhan V, Singh A, Waheed SM, Singh S, Bhatnagar R. Constitutive expression of protective antigen gene of Bacillus anthracis in Escherichia coli. *Biochem Biophys Res Commun*. 2001;283(2):308–315. doi:10.1006/bbrc.2001.4777
9. Krishnanchettiar S, Sen J, Caffrey M. Expression and purification of the Bacillus anthracis protective antigen domain 4. *Protein Expr Purif*. 2003;27(2):325–330. doi:10.1016/S1046-5928(02)00612-5
10. Glenny A, Buttle G, Stevens MF. Rate of disappearance of diphtheria toxoid injected into rabbits and guinea-pigs: toxoid precipitated with alum. *J Pathol Bacteriol*. 1931;34(2):267–275. doi:10.1002/(ISSN)1555-2039
11. Ghimire TR. The mechanisms of action of vaccines containing aluminum adjuvants: an in vitro vs in vivo paradigm. *Springerplus*. 2015;4(1):181. doi:10.1186/s40064-015-0972-0
12. Watkinson A, Soliakov A, Ganesan A, et al. Increasing the potency of an alhydrogel-formulated anthrax vaccine by minimizing antigen-adjuvant interactions. *Clin Vaccine Immunol*. 2013;20(11):1659–1668. doi:10.1128/CVI.00320-13
13. Hansen B, Sokolovska A, HogenEsch H, Hem SL. Relationship between the strength of antigen adsorption to an aluminum-containing adjuvant and the immune response. *Vaccine*. 2007;25(36):6618–6624. doi:10.1016/j.vaccine.2007.06.049
14. Li X, Aldayel AM, Cui Z. Aluminum hydroxide nanoparticles show a stronger vaccine adjuvant activity than traditional aluminum hydroxide microparticles. *J Control Release*. 2014;173:148–157. doi:10.1016/j.jconrel.2013.10.032
15. Iyer S, Robinett RR, HogenEsch H, Hem SL. Mechanism of adsorption of hepatitis B surface antigen by aluminum hydroxide adjuvant. *Vaccine*. 2004;22(11–12):1475–1479. doi:10.1016/j.vaccine.2003.10.023
16. Ribeiro S, Rijpkema SG, Durrani Z, Florence AT. PLGA-dendron nanoparticles enhance immunogenicity but not lethal antibody production of a DNA vaccine against anthrax in mice. *Int J Pharm*. 2007;331(2):228–232. doi:10.1016/j.ijpharm.2006.11.063
17. Manayani DJ, Thomas D, Dryden KA, et al. A viral nanoparticle with dual function as an anthrax antitoxin and vaccine. *PLoS Pathog*. 2007;3(10):e142. doi:10.1371/journal.ppat.0030142
18. Kachura MA, Hickle C, Kell SA, et al. A CpG-Ficoll nanoparticle adjuvant for anthrax protective antigen enhances immunogenicity and provides single-immunization protection against inhaled anthrax in monkeys. *J Immunol*. 2016;196(1):284–297. doi:10.4049/jimmunol.1501903
19. Malik A, Gupta M, Mani R, Gogoi H, Bhatnagar R. Trimethyl chitosan nanoparticles encapsulated protective antigen protects the mice against anthrax. *Front Immunol*. 2018;9:562. doi:10.3389/fimmu.2018.00562
20. Kamaly N, Yameen B, Wu J, Farokhzad OC. Degradable controlled-release polymers and polymeric nanoparticles: mechanisms of controlling drug release. *Chem Rev*. 2016;116(4):2602–2663. doi:10.1021/acs.chemrev.5b00346
21. Du J, Zhang YS, Hobson D, Hydbring P. Nanoparticles for immune system targeting. *Drug Discov Today*. 2017;22(9):1295–1301. doi:10.1016/j.drudis.2017.03.013
22. Kanchan V, Panda AK. Interactions of antigen-loaded polylactide particles with macrophages and their correlation with the immune response. *Biomaterials*. 2007;28(35):5344–5357. doi:10.1016/j.biomaterials.2007.08.015
23. Fifis T, Gamvrellis A, Crimeen-Irwin B, et al. Size-dependent immunogenicity: therapeutic and protective properties of nano-vaccines against tumors. *J Immunol*. 2004;173(5):3148–3154. doi:10.4049/jimmunol.173.5.3148
24. Ruwona TB, Xu H, Li X, Taylor AN, Shi Y-C, Cui Z. Toward understanding the mechanism underlying the strong adjuvant activity of aluminum salt nanoparticles. *Vaccine*. 2016;34(27):3059–3067. doi:10.1016/j.vaccine.2016.04.081
25. Sun B, Ji Z, Liao Y-P, et al. Engineering an effective immune adjuvant by designed control of shape and crystallinity of aluminum oxyhydroxide nanoparticles. *ACS Nano*. 2013;7(12):10834–10849. doi:10.1021/nn404211j
26. Li X, Hufnagel S, Xu H, et al. Aluminum (oxy) hydroxide nanosticks synthesized in bicontinuous reverse microemulsion have potent vaccine adjuvant activity. *ACS Appl Mater Interfaces*. 2017;9(27):22893–22901. doi:10.1021/acsami.7b03965
27. Orr MT, Khandhar AP, Seydoux E, et al. Reprogramming the adjuvant properties of aluminum oxyhydroxide with nanoparticle technology. *NPJ Vaccines*. 2019;4(1):1. doi:10.1038/s41541-018-0094-0
28. Murphy KM, Heimberger AB, Loh DY. Induction by antigen of intrathymic apoptosis of CD4+ CD8+ TCRlo thymocytes in vivo. *Science*. 1990;250(4988):1720–1723. doi:10.1126/science.2125367
29. Brewer JM, Conacher M, Hunter CA, Mohrs M, Brombacher F, Alexander J. Aluminium hydroxide adjuvant initiates strong antigen-specific Th2 responses in the absence of IL-4-or IL-13-mediated signaling. *J Immunol*. 1999;163(12):6448–6454.
30. Mori A, Oleszycka E, Sharp FA, et al. The vaccine adjuvant alum inhibits IL-12 by promoting PI3 kinase signaling while chitosan does not inhibit IL-12 and enhances Th1 and Th17 responses. *Eur J Immunol*. 2012;42(10):2709–2719. doi:10.1002/eji.201242372
31. Oleszycka E, McCluskey S, Sharp FA, et al. The vaccine adjuvant alum promotes IL-10 production that suppresses Th1 responses. *Eur J Immunol*. 2018;48:705–715. doi:10.1002/eji.201747150
32. Li H, Willingham SB, Ting JP-Y, Re F. Cutting edge: inflammasome activation by alum and alum's adjuvant effect are mediated by NLRP3. *J Immunol*. 2008;181(1):17–21. doi:10.4049/jimmunol.181.1.17
33. Fritz JH, Ferrero RL, Philpott DJ, Girardin SE. Nod-like proteins in immunity, inflammation and disease. *Nat Immunol*. 2006;7(12):1250. doi:10.1038/ni1412
34. Kool M, Soullié T, van Nimwegen M, et al. Alum adjuvant boosts adaptive immunity by inducing uric acid and activating inflammatory dendritic cells. *J Exp Med*. 2008;205(4):869–882. doi:10.1084/jem.20071087
35. Hsu PH, Bates TF. Formation of X-ray amorphous and crystalline aluminum hydroxides. *Mineral Mag*. 1964;33(264):749–768.
36. Mani R, Gupta M, Malik A, et al. Adjuvant potential of poly-α-l-glutamine from the cell wall of mycobacterium tuberculosis. *Infect Immun*. 2018;86(10):e00537–00518. doi:10.1128/IAI.00537-18
37. Seeber SJ, White JL, Hem SL. Predicting the adsorption of proteins by aluminium-containing adjuvants. *Vaccine*. 1991;9(3):201–203. doi:10.1016/0264-410X(91)90154-X
38. Gogoi H, Mani R, Bhatnagar R. A niosome formulation modulates the Th1/Th2 bias immune response in mice and also provides protection against anthrax spore challenge. *Int J Nanomedicine*. 2018;13:7427. doi:10.2147/IJN.S153150